SUPPORTING INFORMATION

Evaluation of the subtle trade-off between physical stability and thermo-responsiveness in crosslinked methylcellulose hydrogels

Lorenzo Bonetti,[a] Luigi De Nardo,[ab] Fabio Variola,[c] Silvia Farè[*ab]

[a] Department of Chemistry, Materials and Chemical Engineering "G. Natta", Politecnico di Milano, Piazza Leonardo da Vinci 22, 20133, Milan, Italy.

[b] National Interuniversity Consortium of Materials Science and Technology (INSTM), 50121 Florence, Italy.

[c] Department of Mechanical Engineering, University of Ottawa, Ottawa, ON, K1N 6N5, Canada.

Supporting Information 1

Experimental design (DOE) approach used to study the response of the MC hydrogels in terms of equilibrium swelling (Y), based on three independent factors: CA content (x_1), time (x_2), and temperature (x_3) of the thermal treatment. A face-centered, central composite design (Figure S 1) with 20 runs and 4 center points (Table S 1) was adopted to homogeneously explore the test domain.
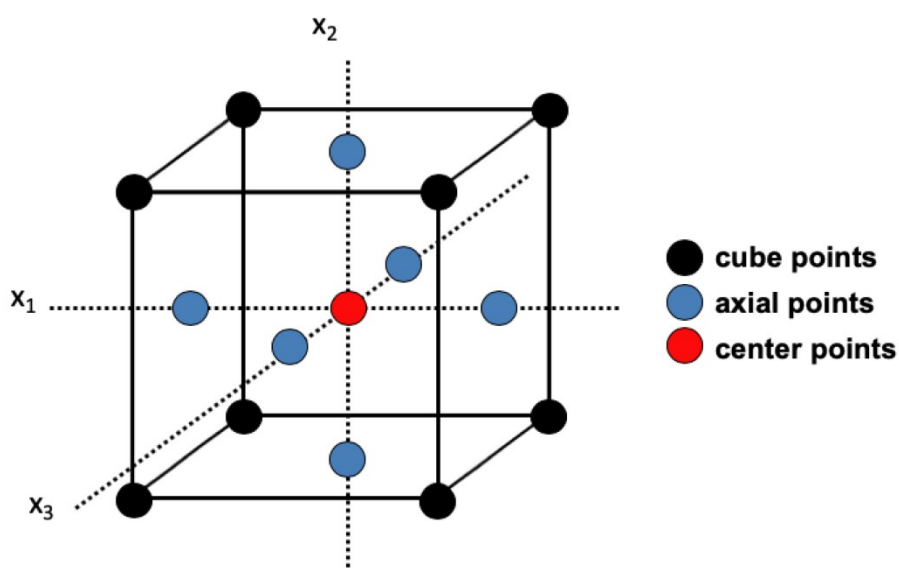

Figure S 1 – DOE space and points used for the face-centered central composite design.

Table S 1 – Natural and coded variables for MC-based samples. Two blocks were identified, since the crosslinking was carried out in two different days. Samples are sorted in order of testing. Center points are here highlighted.

Sample		Natural variables			Coded variables		
RunOrder	Blocks	[CA] (%)	T (°C)	t (min)	x_1	x_2	x_3
1	1	5	190	1	1	1	-1
2	1	5	190	15	1	1	1
3	1	3	177,5	8	0	0	0
4	1	1	165	1	-1	-1	-1
5	1	1	165	15	-1	-1	1
6	1	3	177,5	8	0	0	0
7	1	1	190	15	-1	1	1
8	1	3	177,5	8	0	0	0
9	1	1	190	1	-1	1	-1
10	1	5	165	15	1	-1	1
11	1	3	177,5	8	1	0	0
12	1	5	165	1	1	-1	-1
13	2	3	165	8	0	-1	0

14	2	3	177,5	15	0	0	1
15	2	5	177,5	8	1	0	0
16	2	3	177,5	1	0	0	-1
17	2	3	177,5	8	0	0	0
18	2	3	177,5	8	0	0	0
19	2	1	177,5	8	-1	0	0
20	2	3	190	8	0	1	0

Table S 2 – Swelling rate for MC-based samples tested in the design of experiment (DOE)

Sample	SW (%)
1	7797,77
2	508,34
3	2881,23
4	5650,51
5	5116,17
6	2417,04
7	2729,7
8	2822,22
9	5503,98
10	1851,49
11	2665,81
12	6517,44
13	1870,01
14	1770,23
15	1914,55
16	4634,88
17	2282,97
18	2045,55
19	3579,24
20	1620,84

a

Versus Fits
(response is SW (%))

b
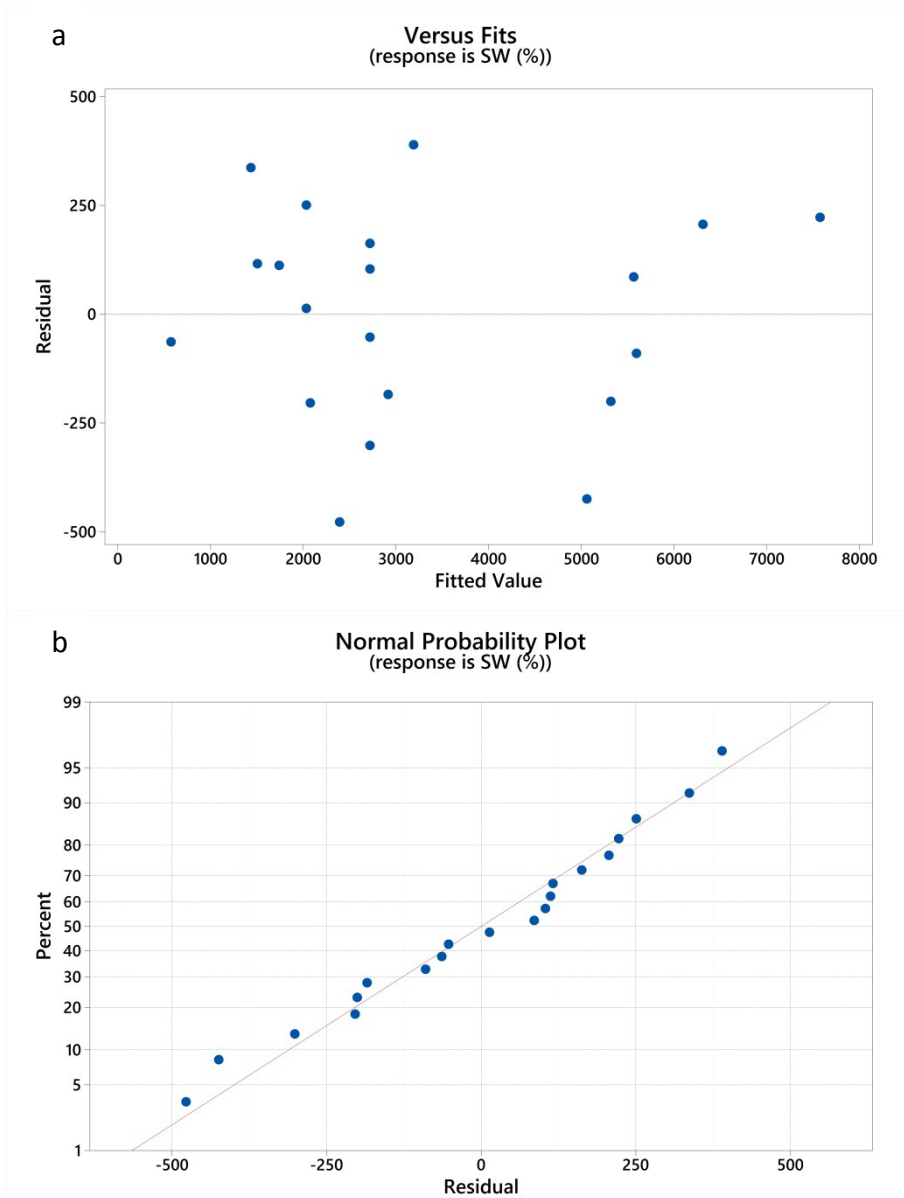
Normal Probability Plot
(response is SW (%))

Figure S 2 – a) Residual plot shows randomly dispersed points around the horizontal axis, meaning that the regression model is appropriate for the data. b) Normal probability plot shows a good linearity, signifying normally distributed data and confirming the validity of the model.
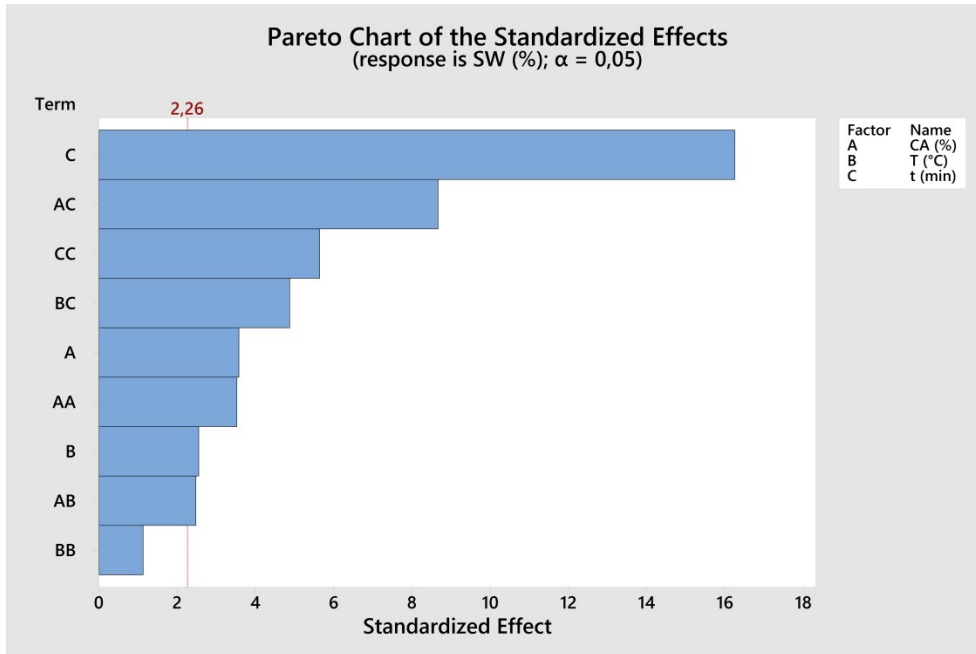
Figure S 3 – The Pareto chart indicates the absolute values of the effects, from the largest to the smallest one. The red line represents a threshold that separates the influencing and the non-influencing effects (α = 0.05)

Supporting Information 2

The calculation of the average molecular weight between crosslinks ($\bar{M}_c$), crosslinking density (ρ_c) and mesh size (ξ) was based on the Flory-Rehner model[1–3].

The equilibrium weight swelling ratio, Q_w, was measured for each crosslinking condition. Hydrogels were incubated in dH_2O at 37 °C until the equilibrium plateau was reached (*i.e.,* 24 h, assumed when no significant differences in the swelling values among two subsequent time points were detectable). Q_w was calculated with equation (1s):

$$Q_w = \frac{w_s}{w_d}$$
(1.s)

where w_s and w_d are the weights of MC in swollen and dried state, respectively[3,4].

The volumetric swelling ratio (Q_v) was calculated from Q_w as follows:

$$Q_v = 1 + \left(\frac{\rho_p}{\rho_s}(Q_w - 1) \right)$$
(2.s)

where ρ_p is the density of the dry MC polymer (0.276 g cm^{-3})[5] and ρ_s is the density of the solvent (1 g cm^{-3} for water).

$\bar{M}_c$ was calculated using the equation (3.s)[2,3]:

$$Q_v^{5/3} \cong \frac{\bar{v}\bar{M}_c}{V_l}\left(\frac{1}{2} - \chi \right)$$
(3.s)

where $\bar{v}$ is the specific volume of the dry polymer, V_l is the molar volume of the solvent (18 mol cm^{-3} for water) and χ is the Flory polymer-solvent interaction parameter. In particular, χ was estimated to be equal to 0.473, comparable to that of other polysaccharides (*e.g.,* dextran, hyaluronic acid), because of the similar chemical structure[3]. Differences between non-crosslinked and crosslinked polymers were assumed to be negligible in the estimation of the χ parameter, as reported elsewhere[2,3,6].

The effective crosslinking density (ρ_c) was calculated as in equation (4.s)[2,3]:

$$\rho_c = \frac{1}{\bar{v}\bar{M}_c}$$
(4.s)

The swollen hydrogel mesh size (ξ) was estimated according to the equation (5.s)[2,3,7]:

$$\xi = Q_v^{1/3}\sqrt{\overline{r_0^2}} \quad \text{(5.s)}$$

where $\sqrt{\overline{r_0^2}}$ is the root-mean square distance between crosslinks and depends on the molecular weight between crosslinks ($\overline{M}_c$). For carboxymethylcellulose (CMC), having a backbone similar to the one of MC, the following equation was previously reported[3,8,9]:

$$\sqrt{\frac{\overline{r_0^2}}{2n}} \cong 2.1 \quad \text{(6.s)}$$

where n is the degree of polymerization at a given molecular weight. As for MC used in this work, with a molecular weight of 88 kDa, $n \cong 471$, it is possible to derive the following equation[3]:

$$\sqrt{\overline{r_0^2}} \cong 0.217\sqrt{M_n} \quad \text{(7.s)}$$

By combining Eqs. (5.s) and (7.s) and by substituting M_n with $\overline{M}_c$, the mesh size can be calculated as:

$$\xi = 0.217\sqrt{\overline{M}_c}Q_v^{1/3} \quad \text{(8.s)}$$

The main parameters which define the microstructure of a crosslinked hydrogel network, namely the average molecular weight between crosslinks ($\overline{M}_c$), the crosslinking density (ρ_c) and the mesh size (ξ), were calculated from equilibrium swelling tests and displayed in Figure S 4. A decrease in the $\overline{M}_c$ ($1.50*10^4 \pm 7.96*10^2$ g mol^{-1} and $1.12*10^3 \pm 3.33*10^2$ g mol^{-1} for MC and MC-H, respectively, Figure S 4a) and an increase in the crosslinking density ($[0.18 \pm 0.01]*10^{-4}$ mol cm^{-3} and $[2.58 \pm 0.65]*10^{-4}$ mol cm^{-3} for MC and MC-H, respectively, Figure S 4b) from not crosslinked (MC) to high crosslinked MC hydrogels (MC-H) can be observed. The mesh size, also referred to as pore size in the macromolecular network and associated with the distance between adjacent crosslinking points, also decreases increasing the crosslinking degree. Specifically, MC-H gels exhibit the lowest ξ values (92.21 ± 5.20 nm) with respect to the MC control (155.50 ± 1.67 nm).

The $\overline{M}_c$, ρ_c and ξ values obtained in this work can be compared with the ones obtained for MC hydrogels crosslinked using reduction-oxidation (redox) initiators systems[3,10]. In particular, ξ values

obtained in the present work resulted higher than the ones obtained for ammonium persulfate (APS)-ascorbic acid (AA) crosslinked MC hydrogels (*i.e.*, $\xi \approx 40 - 80$ nm) and the ones obtained for APS-TEMED crosslinked MC hydrogels (*i.e.*, $\xi \approx 30 - 70$ nm). This can be explained by differences in the polymer concentration and molecular weight, and by the different length and architecture of the crosslinkers used, which imply different extent of crosslinking (*i.e.*, different mesh size of the hydrogels).

The mesh size dimensions control the diffusion rate, defining a dimensional constraint for the possible diffusion of a molecule in or out of the hydrogel network[11]. The prospect of fine tuning ξ values is a fundamental prerequisite for CA crosslinked MC hydrogels as platforms for drug delivery. In this regard, CA crosslinked MC hydrogels displayed ξ values close to the typical range of micro-porous gels (*i.e.*, $\xi = 10 - 100$ nm)[12].
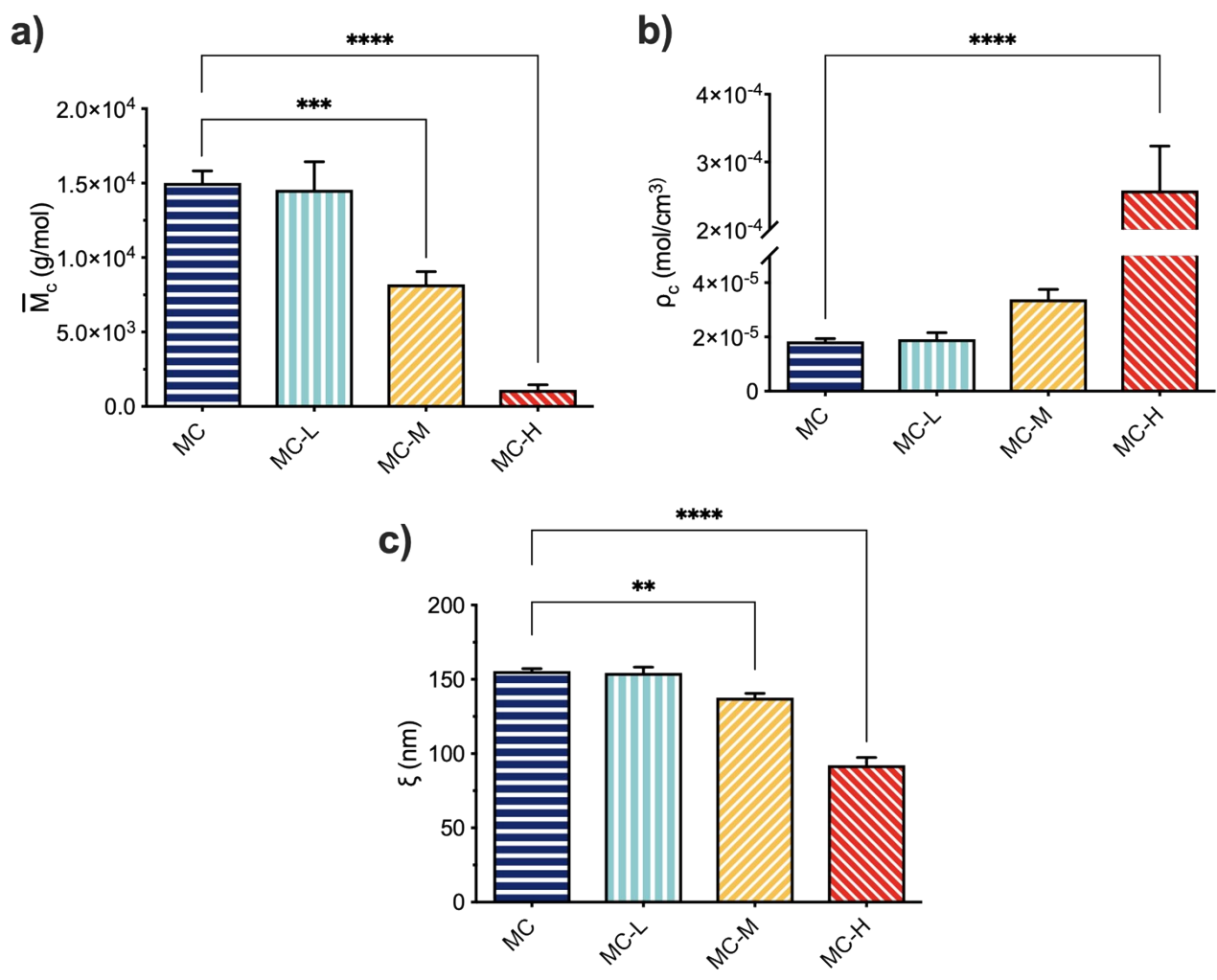
Figure S 4 - Calculated physical parameters of MC hydrogels: a) average molecular weight between crosslinks ($\overline{M}_c$), b) crosslinking density (ρ_c), c) mesh size (ξ). **p<0.01, ***p<0,001, ****p<0,0001.

Supporting Information 3

Thermogravimetric analysis (TGA, PerkinElmer SDA 6000) was performed on pristine MC and CA-crosslinked MC dry samples (MC-L, MC-M, MC-H). Samples were heated from 35 to 800 °C with a heating rate of 10 °C min^{-1}, under nitrogen atmosphere. The main obtained thermal parameters were the initial decomposition temperature (IDT), the temperature at 50% of material decomposition ($D_{1/2}$), the residue at 400 °C ($R_{400°C}$), and the final residue (FR).

Thermogravimetric analysis of dry MC films is reported in Figure S 5. TGA curves show a first weight loss attributable to the evaporation of water (*i.e.,* free and bound) from the polymer in the range 100-200 °C. Between 240 and 400 °C, the decrease in mass can be related to the decomposition of the polymer backbone[13,14]. No differences in the IDT (Table S 4) values were observed among the samples. Interestingly, the thermal stability of MC films was improved by CA crosslinking, as it is possible to observe from the residual weight at 400 °C (after the decomposition phase of the polymer) that increased of about 28 % (Table S 3) between the non-crosslinked films (MC) and the highly crosslinked ones (MC-H). These observations are in agreement with previously published data about other cellulose-derived materials (i.e., CMC and HEC) and starch[13,15,16]. A decrease in the $D_{1/2}$ values (Table S 3) was observed by increasing the crosslinking degree. This means that the crosslinked samples showed a higher weight loss than the non-crosslinked ones between 240 and 400 °C, as observed elsewhere[14,17]. Specifically, for starch films crosslinked with CA a lower degradation temperature ($D_{1/2}$) with respect to non-crosslinked films was attributed to thermal degradation of some of the starch molecules in the crosslinked films, induced by the high curing temperatures needed for the crosslinking reaction to occur[14]. Additionally, for CA crosslinked CMC-based hydrogels the decrease in the $D_{1/2}$ values with respect to the non-crosslinked samples was attributed the reduction in the remaining hydrogen bonds of CMC caused by the esterification reactions that occur with crosslinking[17].
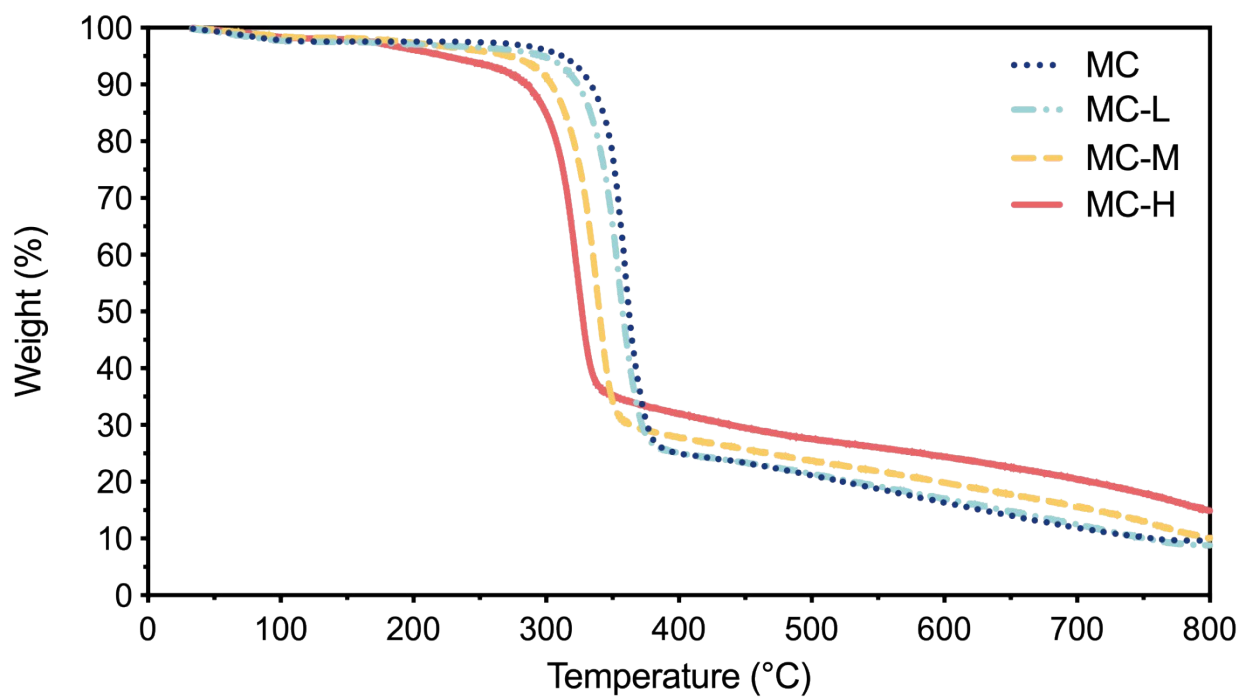
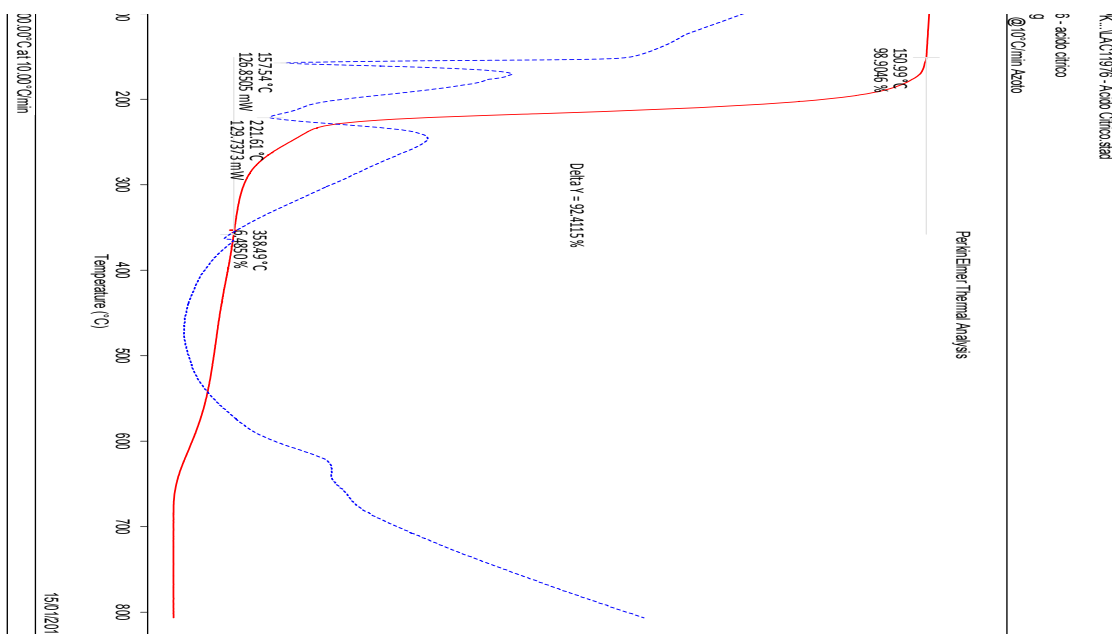Figure S 5 – TGA thermogram of MC films

Figure S 6 – TGA/DTA thermogram of CA powder

Table S 3 - Thermal parameters from TGA analysis on MC films. IDT = initial decomposition temperature; $D_{1/2}$ = temperature at 50 % of material decomposition; $R_{400°C}$ = residue at 400 °C; FR = final residue.

Sample	IDT (°C)	$D_{1/2}$ (°C)	$R_{400°C}$ (%)	FR (%)
MC	243.46	362.27	25.01	9.63
MC-L	241.04	357.6	25.07	8.76
MC-M	241.04	340.09	27.82	9.75
MC-H	241.99	326.88	31.98	14.40

Supporting Information 4

i.   Baseline correction

Linear interpolation method was used for baseline correction (Figure S 7) using the OriginPro software (OriginLab corporation, United States). In particular, 10 anchor points were selected, and subtraction was carried out on all spectra using the same baseline. This procedure was executed to avoid any variability dependence on the spectra processing phase.
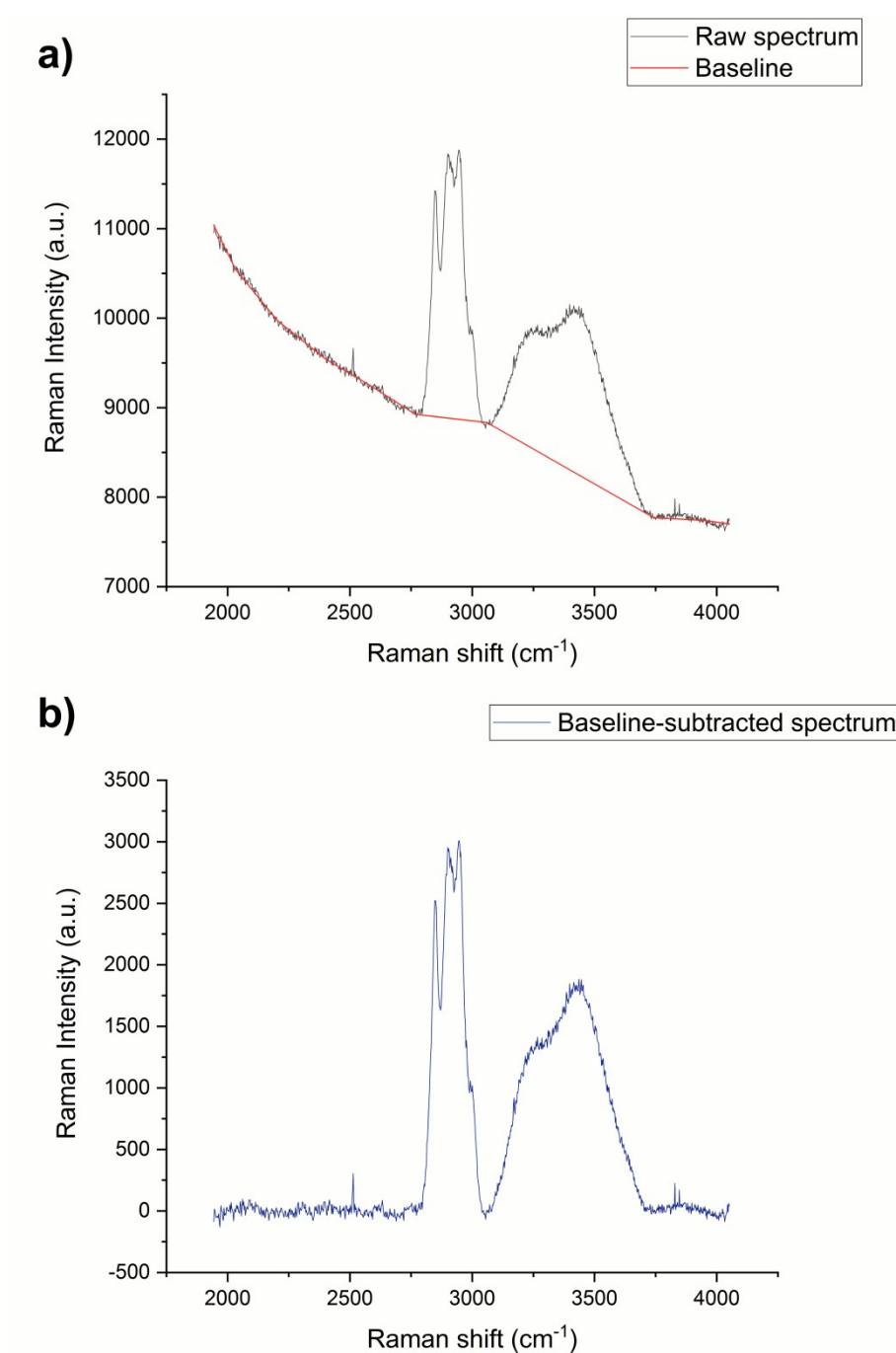

Figure S 7 – a) Representative Raman spectrum before baseline correction (black line) and baseline (red line). b) Representative Raman spectrum after baseline correction (blue line).

ii.   Water-polymer interactions

Water-polymer interactions studies around the LCST of MC were carried out by Raman Spectroscopy. Four sub bands centered at about 2850, 2906, 2952, 2998 cm^{-1} were assigned to asymmetric and symmetric vibrations of methyl groups, and labeled as $v_s(CH_3)$, $v(CH)$, $v_{as}(CH_2)$ and $v_{as}(CH_3)$. The kinetics of volume phase transition around the LCST of MC samples were monitored from the variations in the intensities of C-H$_x$ peaks with the increase of the temperature (Figure S 8).

The intensities of the C-H$_x$ peaks, normalized against the intensity of the peak centered at about 3410 cm-1 (O-H stretching vibration of water), were then plotted as a function of temperature, and a 4PL curve fit was applied (where possible) to the experimental data (Figure S 9).
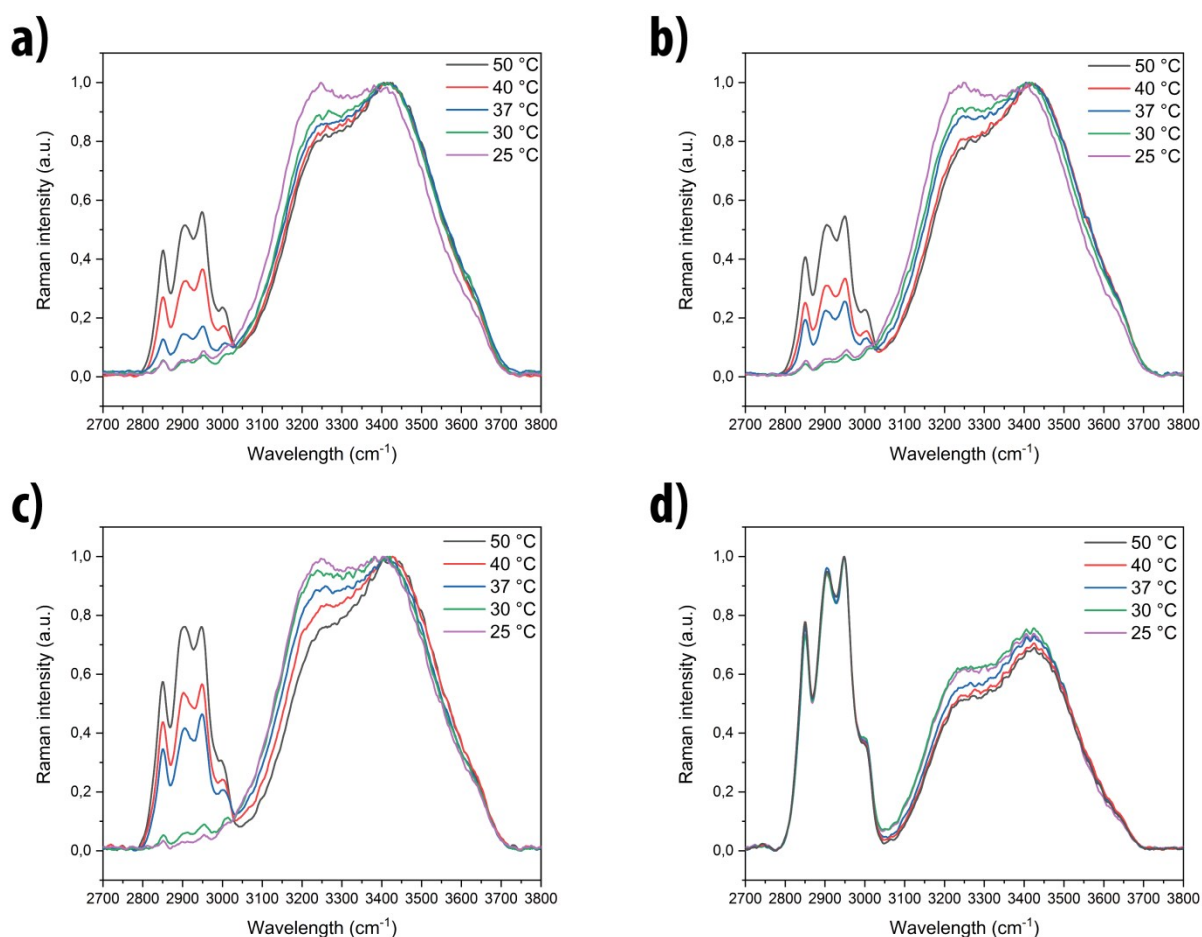

Figure S 8 - Representative Raman spectra, in the region 2700-3800 cm^{-1}, of a) MC, b) MC-L, c) MC-M and d) MC-H hydrogels, swollen in dH$_2$O at the test temperature (25, 30, 37, 40, 50 °C).
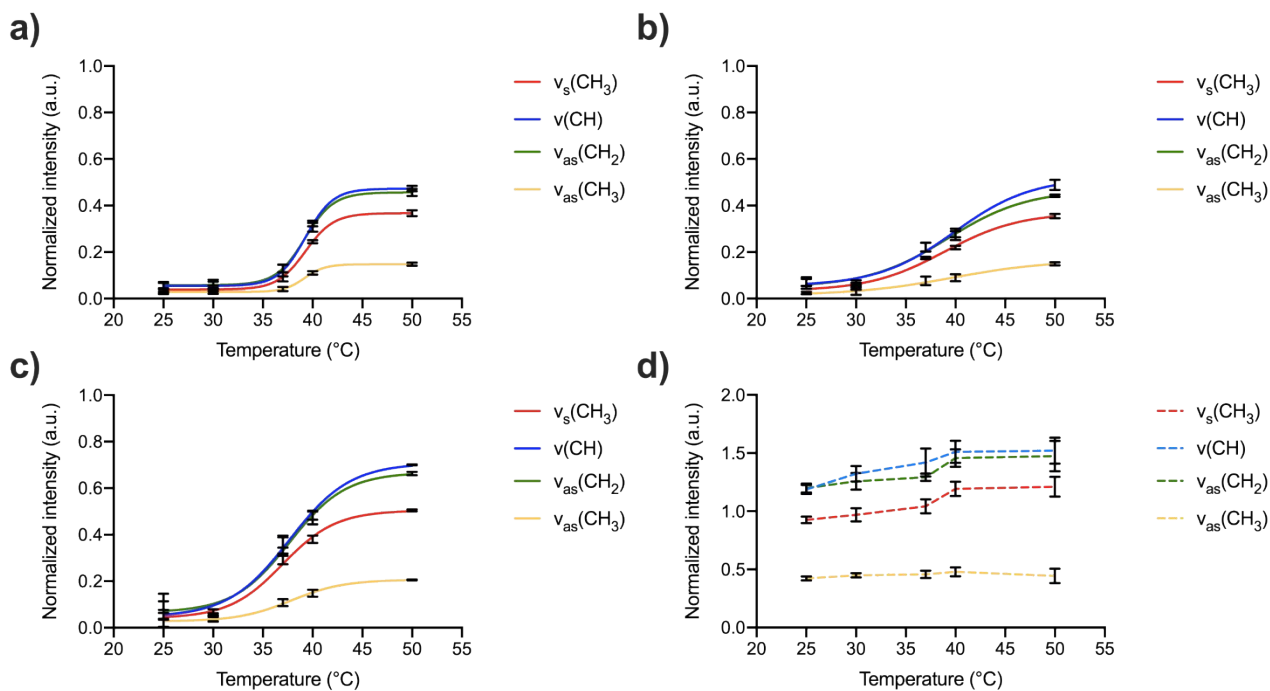
Figure S 9 - Intensities of $v_s(CH_3)$, $v(CH)$, $v_{as}(CH_2)$ and $v_{as}(CH_3)$ bands, as a function of temperature, for a) MC, b) MC-L, c) MC-M, d) MC-H hydrogels. 4PL curve fitting was applied, were possible (continuous line).

Supporting Information 5

i.   Linear viscoelastic region

The linear viscoelastic region (LVR) was investigated on MC hydrogels at the swelling equilibrium by applying an oscillatory strain in the 0.01 – 10 % range, at 37 °C and 1 HZ frequency. The G' values were constant in the strain range 0.01 - 1 % (dotted line) for all the hydrogels (Figure S 10).
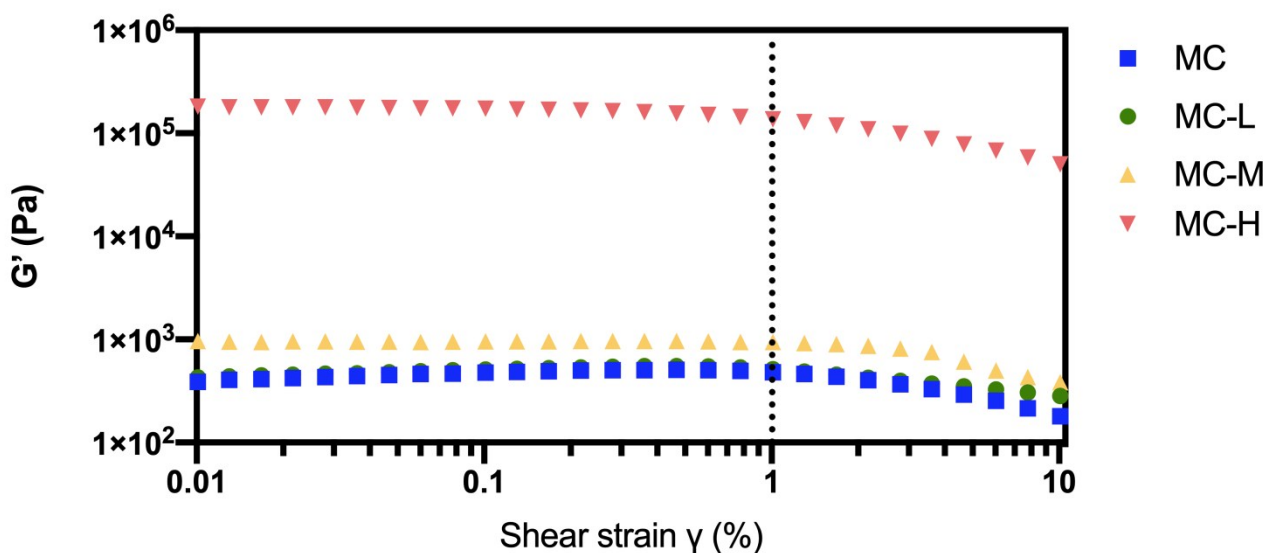

Figure S 10 - Representative storage modulus (G') trend in strain sweep test. LVR was identified in the 0.01 - 1 % shear strain (γ) range (dotted line).

ii.   LCST and heating rate

The heating rate dependency of MC sol-gel transition could be investigated. For a higher accuracy, rates lower than 2 °C min⁻¹ could be explored. However, it should be noted that lower heating rates can result in excessive evaporation, eventually leading to changes in viscoelastic parameters due to a reduced water content in the system (*i.e.*, higher MC concentration)[18].

References:

1   P. J. Flory and J. Rehner, *J. Chem. Phys.*, 1943, **11**, 521–526.
2   J. Baier Leach, K. A. Bivens, C. W. Patrick Jr. and C. E. Schmidt, *Biotechnol. Bioeng.*, 2003, **82**, 578–589.
3   G. T. Gold, D. M. Varma, P. J. Taub and S. B. Nicoll, *Carbohydr. Polym.*, 2015, **134**, 497–507.
4   S. S. Stalling, S. O. Akintoye and S. B. Nicoll, *Acta Biomater.*, 2009, **5**, 1911–1918.
5   M. E. Q. Raymond C R, Paul J S, *Handb. Pharm. excipients, Sixth Ed.*, 2009, 917.
6   K. Gekko, in *Solution Properties of Polysaccharides*, 1981, pp. 415–438.
7   S. J. de Jong, B. van Eerdenbrugh, C. F. van Nostrum, J. J. Kettenes-van den Bosch and W. E. Hennink, *J. Control. Release*, 2001, **71**, 261–275.
8   D. M. Varma, G. T. Gold, P. J. Taub and S. B. Nicoll, *Acta Biomater.*, 2014, **10**, 4996–5004.
9   R. L. Cleland, *Biopolymers*, 1970, **9**, 811–824.
10   G. T. Gold, D. M. Varma, D. Harbottle, M. S. Gupta, S. S. Stalling, P. J. Taub and S. B. Nicoll, *J. Biomed. Mater. Res. Part A*, 2014, **102**, 4536–4544.
11   J. Li and D. J. Mooney, *Nat. Rev. Mater.*, 2016, **1**, 16071.
12   R. Wong, M. Ashton and K. Dodou, *Pharmaceutics*, 2015, **7**, 305–319.
13   K. K. Mali, S. C. Dhawale, R. J. Dias, N. S. Dhane and V. S. Ghorpade, *Indian J. Pharm. Sci.*, 2018, **80**, 657–667.
14   N. Reddy and Y. Yang, *Food Chem.*, 2010, **118**, 702–711.
15   C. Demitri, R. Del Sole, F. Scalera, A. Sannino, G. Vasapollo, A. Maffezzoli, L. Ambrosio and L. Nicolais, *J. Appl. Polym. Sci.*, 2008, **110**, 2453–2460.
16   Y. Seki, A. Altinisik, B. Demircioğlu and C. Tetik, *Cellulose*, 2014, **21**, 1689–1698.
17   N. S. V. Capanema, A. A. P. Mansur, A. C. de Jesus, S. M. Carvalho, L. C. de Oliveira and H. S. Mansur, *Int. J. Biol. Macromol.*, 2018, **106**, 1218–1234.
18   P. Werner, M. Münzberg, R. Hass and O. Reich, *Anal. Bioanal. Chem.*, 2017, **409**, 807–819.